

Accounting for Inks Interaction in the Yule-Nielsen Spectral Neugebauer Model

Silvia Zuffi

ITC, Consiglio Nazionale delle Ricerche, Milano, Italy

Simone Santini

University of California, San Diego, California

and Escuela Politécnica Superior, Universidad Autónoma de Madrid, Madrid, Spain

Raimondo Schettini

DISCo, Università degli Studi di Milano Bicocca, Milano, Italy

Abstract. Multispectral printer characterization requires an effective model to map the inputs to the printer (i.e., the digital counts of the inks) into reflectance spectra and vice versa. Most of the methods for printer modeling are based on the color mixing model of Neugebauer, but this model, in its original formulation, is a rather poor predictor of the printer's output, since it fails to take into account many of the relevant phenomena that take place in the printing process. These phenomena, which include light scattering within the substrate, internal and surface reflection, and ink spreading, determine an enlargement of ink drops called dot gain, which differs on the basis of the substrate condition. This paper presents a novel strategy to model dot gain and interaction among inks in the definition of a printer model based on the Yule-Nielsen spectral Neugebauer equation. The method proposed has been designed for a four-ink ink jet printer, but its formulation is general and may be extended to the characterization of devices having more than four inks. Our method requires the definition of a relatively large number of parameters, that we estimate using genetic algorithms. The model has been tested on two different printers: An Epson Stylus-Color™ 740 ink jet printer and an Epson StylusPhoto™ 890 ink jet printer. Using a data set consisting of 777 samples, regularly distributed in the HSV color space, we have obtained an accuracy in terms of mean root mean squared error of 0.59% and of $1.54 \Delta E_{ab}^*$ for the first printer and of 1.02% and of $2.04 \Delta E_{ab}^*$ for the second printer. With respect to an approach based on a single dot gain function for each ink, our approach based on many dot gain functions reduced the average root mean square error on the test set of about 40% on average. © 2006 Society for Imaging Science and Technology. [DOI: 10.2352/J.ImagingSci.Technol.(2006)50:1(35)]

INTRODUCTION

In recent years, multispectral reproduction has attracted increasing attention because of its appealing feature, compared to colorimetric approaches, of significantly reducing undesirable metamerism effects.¹ In multispectral reproduction the aim is to produce, in print, a color having reflectance equal to that given in input. Multispectral reproduction requires spectral-based printer characterization, that is, a procedure to map the inputs to the printers—which consist of the digital counts of the amounts of different inks to be spread on paper—into reflectance spectra and vice versa. In

this work, we address the problem of accurately modeling a binary printer to predict its spectral outcome given the input digital counts. Binary printers have the capability to deposit only a nominal amount of colorant in any location. To generate colors, halftoning techniques exploiting the low pass filter characteristics of the human eye are used. In the halftoning process, the image plane is partitioned into small areas, each one corresponding to an addressable location (pixel) of the image to be printed; each pixel specifies the value—0 to 100%—of each one of the four colorants (viz., cyan, magenta, yellow, and black) desired at that location. By applying the halftoning process, the number of effective colorant levels is increased at the expense of print resolution. The halftoning schemes commonly used are *rotated screens*, *dot-on-dot screens*, and *stochastic screens*.² In rotated screens, dots for each ink separation plane are placed in similar patterns rotated at different angles, typically 75° for cyan, 15° for magenta, 0° for yellow and 45° for black. On the contrary, dot-on-dot screens place dots for all separations in the same location, on a fixed grid. Stochastic screening follows a different approach: It attempts to minimize the perceived difference between the binary image output and the original continuous tone image, evaluating the perceived error on the basis of the human contrast sensitivity. An important stochastic halftoning approach, first proposed by Floyd and Steinberg in 1975,³ is error diffusion. Characteristic of this approach is that it is not a point process, but depends on the contents of the whole image.⁴ In the modeling of binary printers, the halftoning algorithm is often viewed as a black box, since often a complete control on the placement of dots on the substrate is not possible.

Techniques for spectral-based printer characterization typically use analytical models, formulated on the basis of the physics behind the printing process. Because most theoretical models can only partially describe all the complex phenomena that take place in print, the model's parameters are often determined empirically. Thus, analytical models are a combination of theory and empiricism.⁵ Most of the methods for printer modeling are based on the color mixing

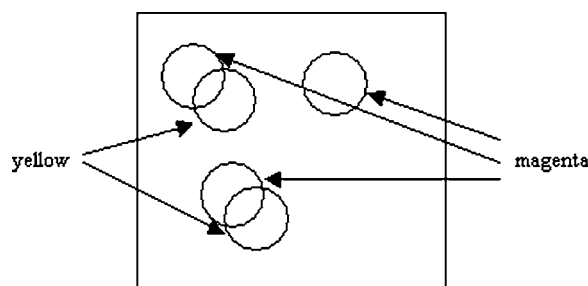


Figure 1. Example of dot placement of two inks, yellow and magenta.

model of Neugebauer.⁶⁻⁹ The model, in its original formulation, is a rather poor predictor of the printer's output, since it fails to take into account many of the relevant phenomena that take place in the printing process. These phenomena include light scattering within the substrate, internal and surface reflection, and ink spreading. The scattering of light and reflections are responsible for what is generally called the *optical dot gain* or the Yule-Nielsen effect. In addition, due to the spreading of the ink on paper, the area of the deposited ink is generally larger than the nominal coverage, yielding a "physical" or "mechanical" dot gain. To take into account the effects of light scattering in the substrate Yule-Nielsen introduced a coefficient known also as the *n*-value. It increases the model's performance, but the resulting Yule-Nielsen spectral Neugebauer model still needs solutions to deal with interactions among inks and of inks with paper. Complex methods have been introduced to describe optical dot gain, among which the convolution with a point spread function (PSF),¹⁰ or probability models.^{11,12} Approaches to describe mechanical dot gain model the diffusion of the ink by enlarging the drop impact on the basis of the configuration of its neighbors and the state of the surface,^{13,14} or by defining a transmission function on a blurred version of the halftone image.¹⁰ An improvement of model accuracy was obtained employing cellular approaches¹⁵ or ascribing partial uncertainty to the measurements of reflectance. Examples of methods that take this circumstance into account are found in Refs. 16 and 17. As the dot gain is the effect of interaction of light and substrate with inks, a complete model for its description should take into account any possible substrate condition, being the "optical" or "mechanical" enlargement of ink drop different depending on whether an ink is deposited on the bare substrate or on previously deposited ink. Strategies to take into account inks interactions have been proposed with a model of ink trapping by Stollnitz et al.,¹⁸ or by Iino and Berns.⁸ Recently, a method to improve the Yule-Nielsen spectral Neugebauer model by dot coverages depending on ink superposition has been proposed by Hersch.¹⁹

In general, many of the strategies proposed starts from an analysis of the print process to define a physical framework for the model. Then, as the physical parameters are difficult if not impossible to measure directly, an optimization phase is carried on. This is the approach that we followed in our work. We have developed a novel method to

describe dot gain and inks interaction in the context of the Yule-Nielsen spectral Neugebauer model, justified by physical considerations and by the analysis of experimental data. Many parameters, to consider any possible condition, are set in an optimization phase. The method proposed has been tested in the modeling of two ink jet printers.

THE YULE-NIELSEN SPECTRAL NEUGEBAUER MODEL

According to the Yule-Nielsen spectral Neugebauer (YNSN) equation, the spectrum of an *N*-inks halftone print is the weighted sum of 2^N different colors, called Neugebauer primaries, given by all the possible overprints of inks. The weight of each Neugebauer primary is the area that the corresponding combination of inks covers in the halftone cell. The YNSN model for a four ink halftone print is

$$R_{\text{print}}(\lambda) = \left[\sum_{p=0}^{15} A_p R_p(\lambda)^{1/n(\lambda)} \right]^{n(\lambda)}, \quad (1)$$

where $R_{\text{print}}(\lambda)$ is the reflectance of the printed color and $R_p(\lambda)$ is the reflectance of the *p*th Neugebauer primary [see Ref. 2 for a detailed description of Eq. (1)]. The wavelength dependent exponent $n(\lambda)$ is the Yule-Nielsen coefficient. In its original formulation, the Yule-Nielsen coefficient is a constant value with a physical meaning: In absence of scattering its value is 1, in case of full scattering its value is 2. In recent work, *n* is considered merely an optimization parameter, and the predictions of the models can be improved by making it a function of the wavelength.^{2,5} In Eq. (1) A_p is the *Neugebauer primary area coverage*, that is the percentage of the halftone cell covered by the *p*th Neugebauer primary. A model commonly used to compute area coverage is Demicheli's, which assumes that drops of ink are placed at random and statistically independent positions inside a "unit cell." This model is considered valid for random or rotated halftone screens,²⁰ while it fails for singular screen superposition, although the color deviation observed is not excessively large.²¹ For dot-on-dot printing a different formulation must be considered.²²

Consider a printer with four inks, cyan, magenta, yellow, and black. If, for a given pixel, the printer only has to deposit one of the inks, then the area covered by it will be proportional to its concentration. If the printer needs to deposit two colors, then the situation is represented schematically in Fig. 1.

Each dot of each color would cover an area proportional to the (fixed) amount of ink that the printer deposits so that, taking the number of dots into account, the overall covered area would still be proportional to the amounts of ink (say *m* and *y*, in this case for magenta and yellow, respectively). There will be, however, some overlap between the two inks. If the pixel is of unitary area and the placement of the dots can be considered random, then the overlap area will be *my*, the area covered by yellow will be *y*(1-*m*), and the area covered by magenta will be *m*(1-*y*). In general, this statistical model predicts that the *Neugebauer primary area coverage* is computed with equations in Table I, that can be

Table I. The calculus of the area coverage according to the Demichel model.

Index, p	Neugebauer primary	Area coverage, A_p
1	K	$(1-c)(1-m)(1-y)k$
2	Y	$(1-c)(1-m)y(1-k)$
3	YK	$(1-c)(1-m)yk$
4	M	$(1-c)m(1-y)(1-k)$
5	MK	$(1-c)m(1-y)k$
6	R	$(1-c)my(1-k)$
7	RK	$(1-c)myk$
8	C	$c(1-m)(1-y)(1-k)$
9	CK	$c(1-m)(1-y)k$
10	G	$c(1-m)y(1-k)$
11	GK	$c(1-m)yk$
12	B	$cm(1-y)(1-k)$
13	BK	$cm(1-y)k$
14	CMY	$cmy(1-k)$
15	CMYK	$cmyk$

summarized with the following equation:

$$A_p = \prod_{i=0}^3 [\text{ind}_{p,i}c_i + (1 - \text{ind}_{p,i})(1 - c_i)], \quad (2)$$

where $p=0, \dots, 15$ is the index of the Neugebauer primary; $\mathbf{c}=[c, m, y, k]$ is a vector with the inks concentrations; $\text{ind}_{p,i}$

is the digit of position i of the index of the primary p , when p is expressed in binary code and the primaries are in the order: White ($\text{ind}_0=[0,0,0,0]$), black ($\text{ind}_1=[0,0,0,1]$), yellow ($\text{ind}_2=[0,0,1,0]$), yellow and black ($\text{ind}_3=[0,0,1,1]$), magenta ($\text{ind}_4=[0,1,0,0]$), magenta and black ($\text{ind}_5=[0,1,0,1]$), red ($\text{ind}_6=[0,1,1,0]$), red and black ($\text{ind}_7=[0,1,1,1]$), cyan ($\text{ind}_8=[1,0,0,0]$), cyan and black ($\text{ind}_9=[1,0,0,1]$), green ($\text{ind}_{10}=[1,0,1,0]$), green and black ($\text{ind}_{11}=[1,0,1,1]$), blue ($\text{ind}_{12}=[1,1,0,0]$), blue and black ($\text{ind}_{13}=[1,1,0,1]$), cyan, magenta and yellow ($\text{ind}_{14}=[1,1,1,0]$), four inks ($\text{ind}_{15}=[1,1,1,1]$).

MODELING DOT GAIN AND INK INTERACTION

The YNSN model is a rather poor predictor of the printer output. Its inaccuracy can mainly be ascribed to the nonlinear relationship—due to the combination of optical and mechanical dot gain—between the theoretical concentration of the ink on paper and its effective concentration (also called effective area). In practice, one must also consider measurement errors, therefore, assuming that the Neugebauer primaries reflectances are subject to uncertainty.^{16,17} In our approach, we consider that the inaccuracy of the YNSN model derives only from errors in the predictions of the inks area coverage. An example of the dot gain effect is indicated in Fig. 2.

The theoretical concentration corresponds to the amount of requested ink, expressed as a fraction of the unit area, as indicated from the digital counts sent to the printer, and the effective concentration is the percentage of area that the dot actually covers in the halftone cell. Usually, the relationship between effective concentration and theoretical concentration is indicated as *dot gain function*. In the paper, we follow this notation, and indicate with *dot gain* the difference between the effective concentration and the theoretical concentration, as in Fig. 2(b). Dot gain, in general, peaks at around 50% of the theoretical concentration. Dot gain functions are commonly used to model the spread of inks

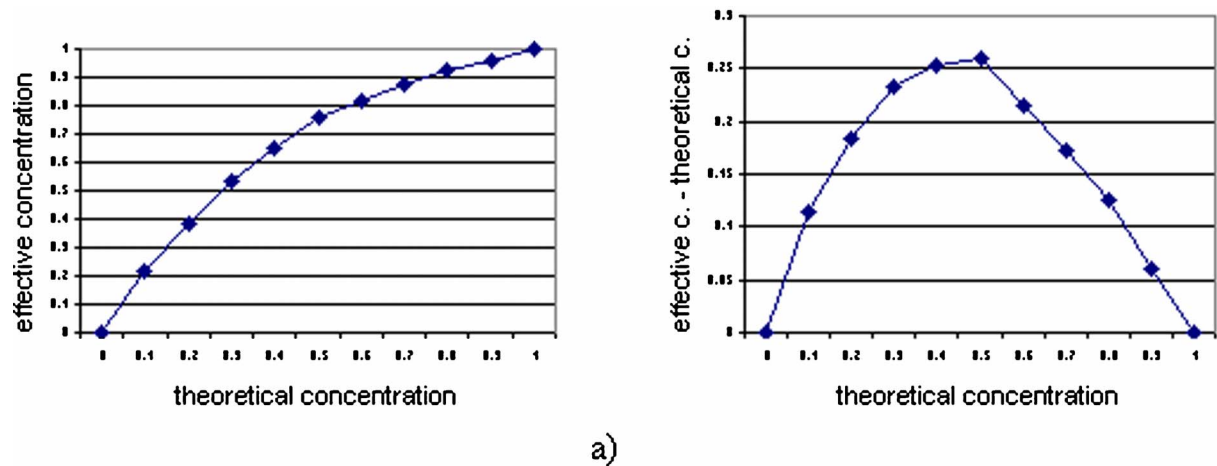


Figure 2. (a) Plot of the effective concentration of ink against theoretical concentration. The plot has been obtained by computing the effective concentration as $1/\Gamma \sum_{\lambda} [(R_{\lambda} - R_{\text{paper},\lambda}) / (R_{\text{ink},\lambda} - R_{\text{paper},\lambda})]$, where Γ is the number of lambda samples, for a ramp of 11 cyan color patches printed with an Epson Stylus Color 740, corresponding to theoretical concentrations regularly distributed in the range $[0, 1]$. (b) Plot of the dot gain of ink against theoretical concentration. Dot gain is computed as difference between the effective and the theoretical concentrations in (a).

Table II. The calculus of the area coverage from effective concentrations of inks. The dependence from theoretical concentration has been omitted for simplicity.

Index, P	Neugebauer primary	Area coverage, A_p
1	K	$(1 - c_{ck})(1 - m_{mk})(1 - y_{yk})k_k$
2	Y	$(1 - c_{cy})(1 - m_{my})y_y(1 - k_{yk})$
3	YK	$(1 - c_{cyk})(1 - m_{myk})y_{yk}k_{yk}$
4	M	$(1 - c_{cm})m_m(1 - y_{my})(1 - k_{mk})$
5	MK	$(1 - c_{cmk})m_{mk}(1 - y_{myk})k_{mk}$
6	R	$(1 - c_{cmy})m_{my}y_{my}(1 - k_{myk})$
7	RK	$(1 - c_{cmyk})m_{myk}y_{myk}k_{myk}$
8	C	$c_c(1 - m_{cm})(1 - y_{cy})(1 - k_{ck})$
9	CK	$c_{ck}(1 - m_{cmk})(1 - y_{cyk})k_{ck}$
10	G	$c_{cy}(1 - m_{cmy})y_{cy}(1 - k_{cyk})$
11	GK	$c_{cyk}(1 - m_{cmyk})y_{cyk}k_{cyk}$
12	B	$c_{cm}m_{cm}(1 - y_{cmy})(1 - k_{cmk})$
13	BK	$c_{cmk}m_{cmk}(1 - y_{cmyk})k_{cmk}$
14	CMY	$c_{cmy}m_{cmy}y_{cmy}(1 - k_{cmyk})$
15	CMYK	$c_{cmyk}m_{cmyk}y_{cmyk}k_{cmyk}$

on paper, and a different dot gain function is defined for each ink. But being the “optical” or “mechanical” enlargement of ink drop different depending on whether the ink is deposited on the bare substrate or on previously deposited ink, a general set of dot gain functions should be dependent from the substrate condition. In this work, we propose to account for the interaction among inks by providing a different dot gain function for any substrate condition. Table II specifies the dot gain functions that have to be considered to compute the area coverage of each Neugebauer primary in Eq. (1). The substrate condition is specified by the pedices, and depends on the inks in the corresponding Neugebauer primary.

Consider, for example, a pixel with theoretical concentration $\mathbf{c}_t = [c_t, m_t, y_t, k_t]$, and suppose that we need to determine the coverage of the Neugebauer primary CK (cyan and black). The CK primary’s area corresponds to the area of the mixture covered by the cyan and black inks, but not by the yellow and magenta. In the probabilistic model, this area would be

$$c_t(1 - y_t)(1 - m_t)k_t. \quad (3)$$

Due to drops overprint, the inks spread on different substrata, and we make the hypothesis that the diffusion process depends on the substratum on which the ink

spreads. In the area of interest for CK, the cyan and black ink are both deposited (if black is not deposited then the area is, of course, part of another primary), so these two inks constitute the substratum on which the diffusion takes place. We are, in other words, interested in the area covered by the diffusion of cyan on a substratum with black, a value that depends on the theoretical concentration of cyan, and that we call $c_{ck}(c_t)$, the two indices being those on the substratum on which the diffusion takes place. Similarly, for the diffusion of the black ink we have $k_{ck}(k_t)$. Consider now the yellow ink: In this case, since yellow is not a component of the Neugebauer primary that we are considering, we are interested in the fraction of the area *not* covered by the ink, that is, one minus the area on the substrate that the yellow covers. But, of course, in the latter area we have not cyan and black, but yellow as well, so the substrate on which the diffusion takes place is not CK, but CYK. We have, in other words, a factor $[1 - y_{cyk}(y_t)]$. So the area of the primary is

$$c_{ck}(c_t)[1 - y_{cyk}(y_t)][1 - m_{cmk}(m_t)]k_{ck}(k_t). \quad (4)$$

Note that, when we talk of *substratum*, we include in it also the ink that is spreading: our function models the diffusion of a specific ink on a specific substratum, so it depends on the ink that is spreading as well as on those on which it is spreading. Note also that each ink that is part of the Neugebauer primary spreads on a substratum composed of the inks of the primary, while each ink that is not part of the primary spreads on a substrate composed of itself plus the inks in the primary. In Table II, for each ink, there are eight possible functions, depending on the presence or absence of the other three ink ($2^3=8$; the substratum on which an ink spreads always includes the ink itself). Considering the calculus of the area coverage of the Neugebauer primary G (green), c_{cy} is now the dot gain function to use, where the subscript “cy” indicates that the substrate is covered by cyan and yellow ink. The same dot gain function, c_{cy} , is used to compute the effective concentration of cyan in the Neugebauer primary Y (yellow), as, if the theoretical concentration of cyan is not zero, then the substrate condition is again presence of cyan and yellow ink. The area of paper coverage is computed as the difference between the sum of the area coverage of the inks and their overprints, with the constraint to be positive:

$$A_0 = 1 - \sum_{p=1}^{15} A_p, \quad A_0 \geq 0. \quad (5)$$

The dot gain functions in Table II, expressing effective concentrations for any substrate condition, have been defined on the basis of a very approximated model of ink diffusion, that we describe in the following. Assume that a drop of ink on the page spreads following the linear diffusion equation:

$$\frac{\partial u}{\partial t} = c \left(\frac{\partial^2 u}{\partial x^2} + \frac{\partial^2 u}{\partial y^2} \right), \quad (6)$$

where c is a diffusion coefficient that depends on the substratum on which the ink is spreading. If the initial condition

at time 0 is given by $g(r, 0) = u(r)$, where $r = \sqrt{x^2 + y^2}$, then the general solution of the diffusion equation is

$$g(r, t) = u(r) * G(r, t) = \int u(q) G(r - q, t) dq, \quad (7)$$

where $G(r, t) = 1 / (4\pi ct) \exp[-r^2 / (4ct)]$ is the Gaussian kernel and $*$ is the convolution operator. The diffusion of the ink can be predicted if the initial shape of the drop that falls on the paper is known. Assuming that the drop itself has the shape of a Gaussian, we represent the initial ink distribution as

$$u(r) = \frac{1}{\pi} \exp\left(-\frac{r^2}{\sigma^2}\right), \quad (8)$$

where σ is a parameter related to the amount of ink that is dropped on the page, given by

$$\frac{1}{\pi} \int \exp\left(-\frac{r^2}{\sigma^2}\right) dx dy = \sigma^2. \quad (9)$$

In the Gaussian function more than 99% of the volume is concentrated in a circle of radius 3σ , which we call *initial radius* of the ink drop. The initial area of the drop $\kappa = 9\pi\sigma^2$ is proportional to the amount of ink. Introducing the parameter $\tau = \sigma^2 / 4c$, the initial condition can be written as

$$g(r, 0) = \frac{1}{4\pi c \tau} \exp\left(-\frac{r^2}{4c\tau}\right), \quad (10)$$

that is, the initial condition is the same that we would have after diffusing a punctiform drop of ink for a time $\tau = \sigma^2 / 4c = \kappa / 4c$. It follows that the solution of the equation is simply the continuation of this diffusion process and the area covered by the ink at time t is

$$a(t) = 36\pi(\tau + t) = 9\pi\sigma^2 + 36\pi ct = \kappa + 36\pi ct. \quad (11)$$

Assuming that the ink maintains its viscosity until the time t_d and then suddenly dries out, the diffusion after a time t_d stops. If we now consider the spread of two inks, supposing that the first ink is sprayed directly on paper (without interacting with any ink already present on the page), the area that it will cover is

$$a_{1,p} = \kappa_{1,p} + 36\pi ct_{d1} = \kappa_{1,p} + \xi_{1,p}, \quad (12)$$

where the subscript p indicates the spread on paper. If we now consider the spread of a second ink, it will expand over the previous ink at a different speed than on paper. This means that the diffusion coefficient must be replaced by $c' = c(1 + \alpha)$,

$$a_{2,1} = \kappa_{2,p} + 36\pi ct_{d2} + 36\pi c\alpha t_{d2} = \kappa_{2,p} + \xi_{2,p} + \xi_{2,1}. \quad (13)$$

Equation (13) expresses the dot gain of an ink on a previous deposited ink as a fixed term $\kappa_{2,p}$ that represents

the amount of deposited ink, related to the theoretical concentration; plus a diffusion term $\xi_{2,p}$ that represents the dot gain on paper; plus a term $\xi_{2,1}$ that represents the dot gain on the previous ink. Note that the last two terms are similar, and differs for a multiplicative constant. The terms $\kappa_{2,p} + \xi_{2,p}$ are the *dot gain function of ink on paper*, that is, the function that relates effective concentration and theoretical concentration. In the following, the term $\xi_{2,1}$ is the *variation of the dot gain* due to a previous ink.

The overlap area, corresponding to the Neugebauer primary area coverage of the inks overprint, therefore will be

$$A_3 = (\kappa_{1,p} + \xi_{1,p})(\kappa_{2,p} + \xi_{2,p} + \xi_{2,1}), \quad (14)$$

where the index of the overprint is indicated as “3” to follow the notation in Table I, where the index in area coverage indicates, in base 2, the inks in the overprint. Note that κ are the quantities of the two inks that are injected on the paper, corresponding to the theoretical concentration, and ξ are coefficients, to be determined experimentally, that represent ink spreading. In summary, in the case of two inks, the areas covered by all possible combinations of two inks are given by

$$A_0 = (1 - a_{1,p})(1 - a_{2,p}) = 1 - A_1 - A_2 - A_3,$$

$$A_1 = a_{1,p}(1 - a_{2,1}), \quad (15)$$

$$A_2 = (1 - a_{1,p})a_{2,p},$$

$$A_3 = a_{1,p}a_{2,1}.$$

Note that the model is asymmetric: it assumes that the sequence of placement of inks on paper is known. If we do not make any assumption about the ink sequence in print, the model can be rewritten in a symmetric form as

$$A_0 = 1 - A_1 - A_2 - A_3,$$

$$A_1 = a_{1,p}(1 - a_{2,1}), \quad (16)$$

$$A_2 = (1 - a_{1,2})a_{2,p},$$

$$A_3 = a_{1,2}a_{2,1}.$$

As described in Eq. (13), the dot gain function of an ink in presence of another ink is a variation of the dot gain function of ink on paper. We need to express this relationship in terms of theoretical ink concentration, in order to compute the effective ink concentration as

$$a_{2,1}(\text{ink}_t) = a_{2,p}(\text{ink}_t) + \xi_{2,1}(\text{ink}_t), \quad (17)$$

where ink_t is the theoretical concentration, one of $\mathbf{c} = [c_t, m_t, y_t, k_t]$. We represent the dot gain function of a single ink on paper, $a_{2,p}(\text{ink}_t)$ in Eq. (16), with a cubic spline function composed by 11 knots. To represent the variations of the dot gain function due to the previous ink, $\xi_{2,1}(\text{ink}_t)$ in Eq. (16), we propose the following empirical function:

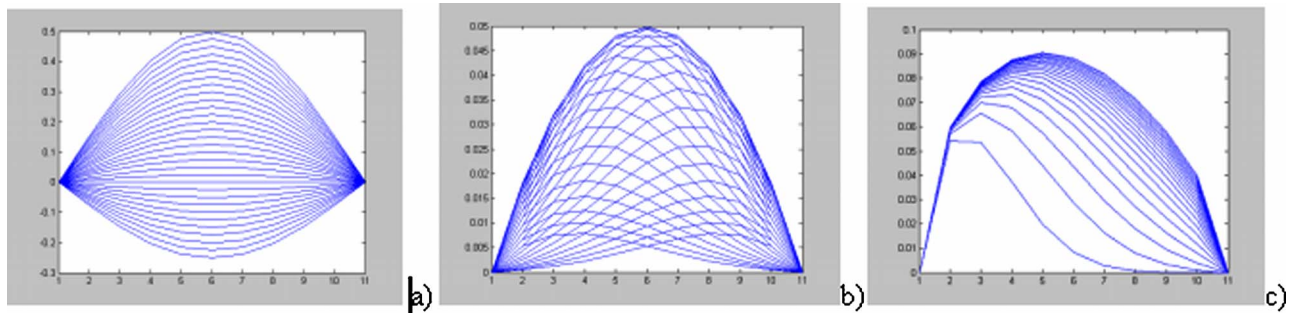


Figure 3. Ink variation model [Eq. (15)] for different values of H (a), μ (b) and s (c).

$$\xi_{2,1}(\text{ink}_t) = H_{2,1} \exp\left(-\frac{(\text{ink}_t - \mu_{2,1})^2}{s_{2,1}}\right) \text{ink}_t(1 - \text{ink}_t) \quad (18)$$

where ink_t is the theoretical concentration, one of $\mathbf{c} = [c_t, m_t, y_t, k_t]$, H , μ , and s are parameters. Plots of Equation (18) for different values of the parameters are shown in Fig. 3. In Eq. (13) we have modeled the variation of dot gain due to a previous ink and the dot gain on paper with similar terms, therefore, in the definition of an empiric function to model $\xi_{2,1}$ as a function of ink_t we looked for a function that can well represent the dot gain of the cyan ink obtained from measurements, reported in Fig. 2(b).

The proposed model considers the variation of dot gain as dependent only on the ink's theoretical concentration: In case of multilayer overprints, the presence of other inks is accounted, as a mean effect, by function parameters that are specific for the type of inks, but independent from their concentrations. It is worth noting that the same approach has been adopted by Tzeng,²³ as a solution to achieve better accuracy with respect to previous proposals that considered the concentrations of secondary inks.⁸

The optical dot gain, theoretically modeled by the Yule-Nielsen coefficient, clearly depends on the characteristics of the substrate and of the ink layers. Values of n may have a

physical meaning for $n < 2$, but, as observed by Viggiano,²⁴ the fringe in the shape of ink dots causes an increase of n , which may go beyond the theoretical limit of 2. In practice, the Yule-Nielsen coefficient is allowed to assume any value that minimizes the accuracy error of the model and is treated as an optimization parameter, regardless of its physical meaning. To improve the model fit, it can also be allowed to vary with the wavelength.² This approach has been followed in our work, while mechanical dot gain functions have been considered wavelength-independent. Increasing the value of n brings a reduction in the spectral match error if no dot gain function is employed to describe effective concentrations. In practice, we assume that the optimization of the wavelength-dependent n -value accounts for optical dot gain, the light scattering being presumably related to wavelength.⁷ The mechanical dot gain, modeled by our dot gain functions, is instead considered wavelength-independent. The n -value and dot gain functions optimization must therefore be performed simultaneously.

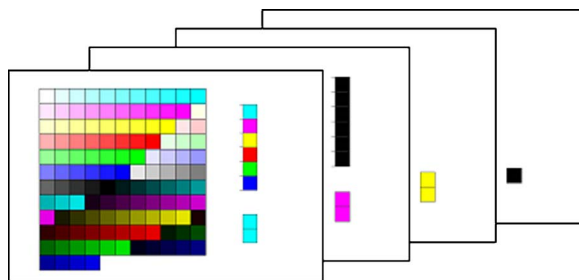


Figure 4. The set of images to obtain measured data for the training phase. The front image must be printed first, and includes the ramp of inks mixtures for model training. The column of patches on the right of training samples includes the patches for overprints measurements. The print of the second image on the same sheet of the first one produces the overprint of black on primary inks and secondary (R,G,B) colors. The print of the third and the last image produce the overprint of the three inks cyan, magenta and yellow, and the overprint of the four inks.

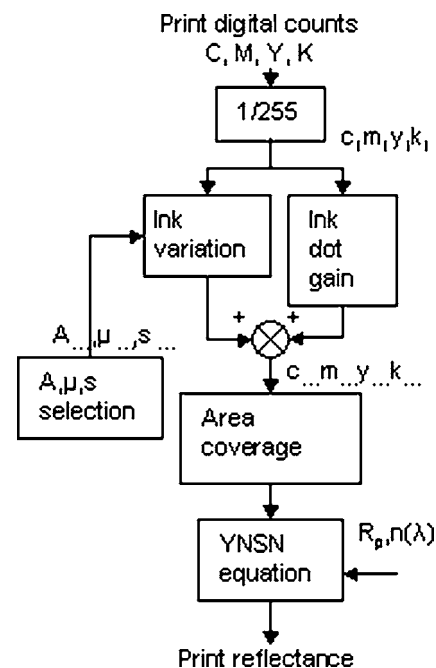


Figure 5. A graphical representation of the model.

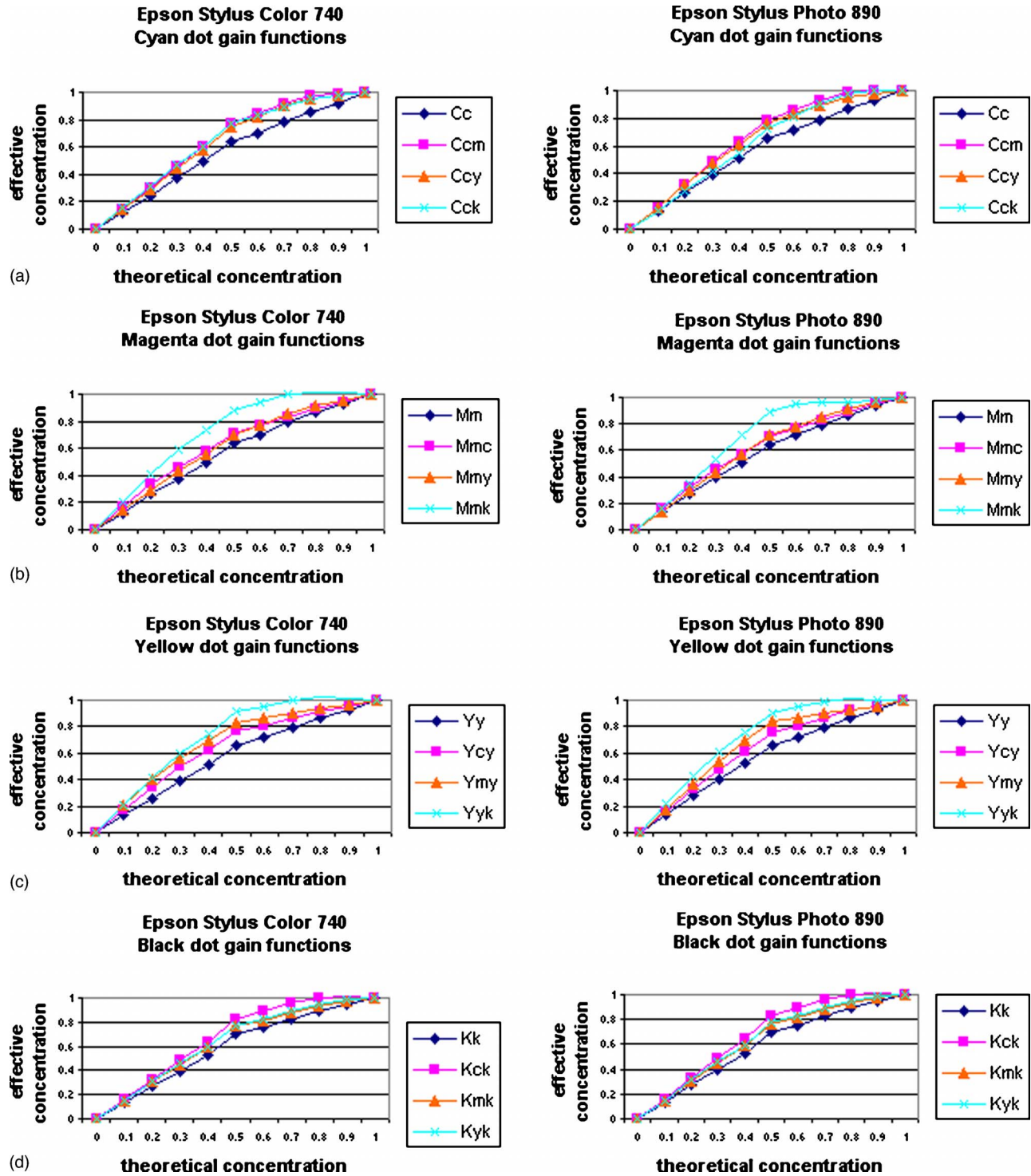


Figure 6. Dot gain functions for the two printers tested for the cyan (a), yellow (b), magenta (c), and black inks (d).

The printer model has a total of 159 parameters: 11 spline knots for each ink to the mechanical represent dot gain function on paper, plus 28×3 parameters to model inks interaction (see Table II), plus the 31 wavelength samples of the Yule-Nielsen coefficient. These parameters are estimated by a model fit optimization phase using genetic algorithms. The cost function to minimize is

$$\text{cost} = \frac{1}{S} \left[\sum_{s=1}^S \frac{1}{\Gamma} \left(\sum_{\lambda=1}^{\Gamma} (R_{\text{print},\lambda,s} - R_{\text{meas},\lambda,s})^2 \right) \right], \quad (19)$$

where S is the number of samples in the training set, Γ is the number of wavelength samples, R_{print} is the reflectance

Table III. Error statistics for the proposed method.

Data Set	ΔE_{ab}^* Avg.	ΔE_{ab}^* 95%	rms% Avg.	rms% Max.	rms% S. dev.
Epson Stylus Color 740					
Training	1.471	4.434	0.495	2.176	0.451
Test	1.541	3.956	0.585	2.397	0.461
Epson Stylus Photo 890					
Training	1.407	4.443	0.499	2.354	0.459
Test	2.040	5.165	1.019	2.932	0.485

computed with the YNSN model [Eq. (1)] and R_{meas} is the measured reflectance of the training set.

EXPERIMENTS

To test the performance of the proposed model, we employed an Epson StylusColor™ 740 and an Epson StylusPhoto™ 890 ink-jet printers. In order to have a complete control over the printer, we replaced the manufacturer's drivers with a Linux driver which generates the ESC/P2 commands to drive both the Epson printers. The Epson StylusPhoto 890 is a six-ink printer, but it was used as a four-ink printer. We used Epson Photo Quality Paper and Floyd Steinberg dithering.

The training set is composed of uniform ramps of eleven patches each, ranging from the absence of ink to full ink coverage of cyan, magenta, yellow, and black. Ramps on secondary colors, red, green, and blue, are also present. In the training set we have also considered patches where primary and secondary colors are printed with black. In these ramps, the theoretical concentration ranges from 1 to 0 for the color and from 0 to 1 for black (for example, in the ramp of cyan with black, the first patch is full cyan ink, the last patch is full black ink and the middle patch has a theoretical concentration of 50% cyan and 50% black). The training set is composed, therefore, of 143 samples. The Neugebauer pri-

maries are obtained by measuring the printed inks at full coverage, and their overprints, by successive prints on the same sheet. In Fig. 4 the training set sheets are illustrated. The page in front, with the 125 patches that constitute the training set (equal patches in the training set are printed and measured once) is printed first. Then, on the same sheet the images in the back are printed in sequence, so the black will cover the six patches of the column on the right (cyan, magenta, yellow, red, green, and blue) to produce the overprints of primaries and secondary colors with black, and the magenta patches will cover the cyan patches. Then, printing the third image, the three-ink overprints are generated. Finally, with the last image, we obtain the four-ink overprint.

The test set consists of 777 samples, regularly distributed in the HSV color space. Measurements of the spectra are executed with a Gretag Spectrolino, considering values in the wavelength range from 400 to 700 nm with a step of 10 nm. In Fig. 5 a graphical representation of the model is reported. For the optimization phase we used the "GAdeme" genetic algorithm in the Galib library.²⁵ The probability of crossover and mutation was set at 0.9 and at 0.002, respectively. Selection was based on the "tournament" method. The genetic algorithm adopted has multiple, independent populations. We considered 10 populations, each one including 10 individuals that were randomly selected; the stopping criterion was the number of iterations performed, that we set at 4000 iterations. The genetic algorithm with parallel populations is computationally very expensive, and the optimization of the many parameters of the printer model took several hours on a Pentium IV PC. The results are reported in terms of color difference in CIELAB ΔE_{ab}^* under the D65 illuminant and root mean square error in Table III.

The optimization process estimates the dot gain functions that globally optimize the rms error on the whole training set. The estimated functions referred to the dot gain of each ink in presence of a second ink are reported in Fig. 6. It can be observed from all the plots that the dot gain function of an ink on paper (the first curve in each legend) is always lower than those obtained in the presence of a second ink, presumably due to paper wetting.

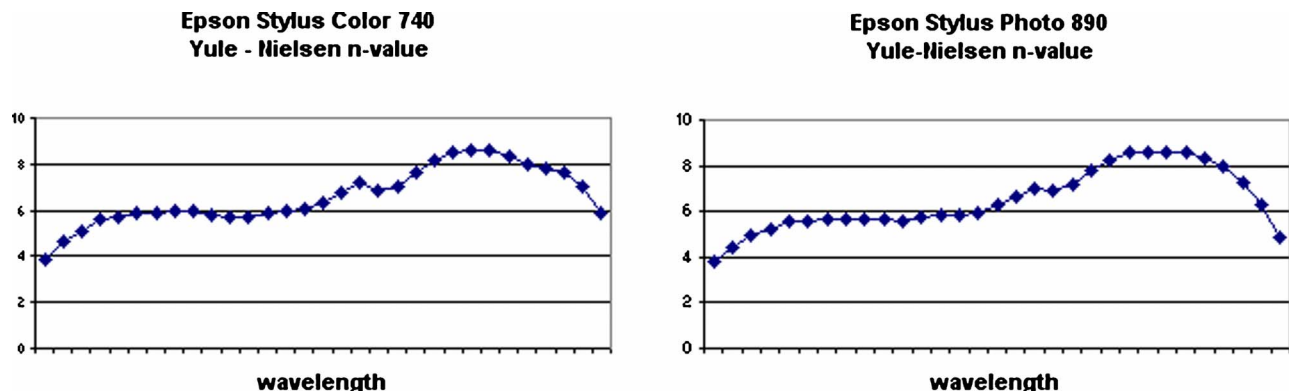


Figure 7. The Yule-Nielsen n -value estimated in the optimization for the Epson StylusColor 740 printer and the Epson StylusPhoto 890 printer.

Table IV. Error statistics when considering a single dot gain function for each ink.

Data set	ΔE_{ab}^* Avg.	ΔE_{ab}^* 95%	rms% Avg.	rms% Max.	rms% S. dev.
Epson Stylus Color 740					
Training	2.232	5.943	1.285	6.706	1.032
Test	2.629	5.500	1.675	5.952	1.033
Epson Stylus Photo 890					
Training	2.057	5.587	0.908	3.579	0.830
Test	2.566	5.876	1.242	4.391	0.698

In Fig. 7, we reported the Yule-Nielsen coefficient resulted from the optimization in the two experiments performed. It can be observed a similar result for both the printers considered. The low values at the extremes of the wavelength range (400–700 nm) are in accordance to results reported from Iino and Berns.⁵

In order to evaluate the advantage in the adoption of many dot gain functions, as proposed in this work, we computed results considering only dot gain functions for single inks. These results are reported in Table IV.

CONCLUSIONS

In this paper we have proposed a method to represent dot gain and interaction among inks in printer modeling using the Yule-Nielsen spectral Neugebauer model. The method requires the definition of a large number of parameters, that have been estimated using genetic algorithms. The feasibility of our approach has been verified in the spectral-based characterization of an ink jet printer producing a spectral accuracy in terms of mean root mean squared error of 0.59% and of 1.54 ΔE_{ab}^* for an Epson StylusColor 740 printer and of 1.02% and of 2.04 ΔE_{ab}^* for an Epson StylusPhoto printer. With respect to an approach based on a single dot gain function for each ink, our approach based on many dot gain functions reduced the average root mean square error on the test set from 1.68 to 0.59 and from 1.24 to 1.02 for the printers considered. In the literature, many strategies have been proposed to improve the accuracy of Neugebauer models. Approaches exist that assumes that the Neugebauer primaries can be optimized, or increased in number to face the problem with cellular methods, that treat the Neugebauer equation as an interpolation model.^{7,15} This last strategy has been adopted in spectral-based characterization applications.²⁶ Despite the fact that a direct comparison of the performance of the methods is not possible, due to the differences in devices and test sets with reported performance,²⁷ we underline that our method is comparable in performance with cellular approaches. A similar conclusion holds for methods based on neural networks.²⁸ With respect to these techniques, however, our method requires printing and measuring a smaller training set.

The model we have proposed is based on assumptions that limit the dependence of an ink dot gain function to the

theoretical concentration of the ink. But a general model should consider dot gain functions dependent from the theoretical concentration of all the printer's inks. This is an extension of our model that we plan to investigate in future research, together with the application of our method to different halftoning screens.

REFERENCES

- ¹B. Hill, "Color capture, color management, and the problem of metamerism: Does multispectral imaging offer the solution?", *Proc. SPIE* **3963**, 2–14 (2000).
- ²D. R. Wyble and R. S. Berns, "A critical review of spectral models applied to binary color printing", *Color Res. Appl.* **25**, 1 (2000).
- ³C. Hains, S. Wang, and K. Knox, "Digital color halftone", in *Digital Color Imaging Handbook*, G. Sharma, Ed. (CRC Press, Boca Raton, FL, 2003) Chap. 6.
- ⁴H. R. Kang, "Digital color halftoning", *SPIE/IEEE Series on Imaging Science and Engineering* (SPIE, Bellingham, WA, 1999).
- ⁵K. Iino and R. S. Berns, "Building color-management modules using linear optimization I. Desktop color systems", *J. Imaging Sci. Technol.* **42**, 79–94 (1998).
- ⁶S. Zuffi and R. Schettini, "Modeling dot gain and inks interaction", in *Proc. IS&T/SID 12th Color Imaging Conference* (IS&T, Springfield, VA, 2004) pp. 181–186.
- ⁷R. Balasubramanian, "Optimization of the spectral Neugebauer model for printer characterization", *J. Electron. Imaging* **8**, 2 (1999).
- ⁸K. Iino and R. S. Berns, "A spectral based model of color printing that compensates for optical interactions of multiple inks", *Proc. 8th Congress International Color Association AIC Color 97*, (The Color Science Association of Japan, Tokyo, Japan, 1997) pp. 610–613.
- ⁹D. Tzeng and R. S. Berns, "Spectral-based six-color separation minimizing metamerism", *Proc. IS&T/SID 8th Color Imaging Conference* (IS&T, Springfield, VA, 2000) pp. 342–347.
- ¹⁰S. Gustavson, "Color gamut of halftone reproduction", *J. Imaging Sci. Technol.* **41**, 283–290 (1997).
- ¹¹J. S. Arney, T. Wu, and C. Blehm, "Modeling the Yule-Nielsen effect on color halftones", *Proc. IS&T/SID 5th Color Imaging Conference* (IS&T, Springfield, VA, 1997) pp. 62–65.
- ¹²J. S. Arney, T. Wu, and C. Blehm, "Modeling the Yule-Nielsen effect on color halftones", *J. Imaging Sci. Technol.* **42**, 4 (1998).
- ¹³P. Emmel and R. D. Hersch, "A unified model for color prediction of halftoned print", *J. Imaging Sci. Technol.* **44**, 4 (2000).
- ¹⁴P. Emmel and R. D. Hersch, "Modeling ink spreading for color prediction", *J. Imaging Sci. Technol.* **46**, 3 (2002).
- ¹⁵A. U. Agar and J. P. Allebach, "An iterative cellular YNSN method for color printer characterization", *Proc. IS&T/SID 6th Color Imaging Conference* (IS&T, Springfield, VA, 1998) pp. 197–200.
- ¹⁶M. Xia, G. Sharma, and A. M. Tekapl, "End-to-end color printer calibration by total least square regression", *IEEE Trans. Image Process.* **8**, 5 (1999).
- ¹⁷C. Lana, M. Rotea, and D. Viassolo, "Characterization of color printers using robust parameter estimation", *Proc. IS&T/SID 11th Color Imaging Conference* (IS&T, Springfield, VA, 2003) pp. 224–231.
- ¹⁸E. J. Stollnitz, V. Ostromoukhov, and D. H. Salesin, "Reproducing color images using custom inks", *Proc. SIGGRAPH'98*, 267–274 (1998).
- ¹⁹R. D. Hersch, "Improving the Yule-Nielsen modified spectral Neugebauer model by dot surface coverages depending on the ink superposition conditions", *Proc. SPIE* **5667**, 434–445 (2005).
- ²⁰G. L. Rogers, "Neugebauer revisited: Random dots in halftone screening", *Color Res. Appl.* **23**, 2 (1998).
- ²¹I. Amidror and R. D. Hersch, "Neugebauer and Demichel: Dependence and independence in n -screen superpositions for color printing", *Color Res. Appl.* **25**, 4 (2000).
- ²²R. Balasubramanian, "Printer model for dot-on-dot halftone screens", *Proc. SPIE* **2413**, 356–364 (1995).
- ²³D. Tzeng, "Spectral-based color separation algorithm development for multiple-ink color reproduction", Ph.D. Thesis (R.I.T., Rochester, NY, 1999).
- ²⁴J. A. S. Viggiano, "Modeling the Color of Multi-Colored Halftones", *Proc. TAGA*, 44–62 (1990).
- ²⁵M. Wall, "GAlib: A C++ library of genetic algorithm components", Massachusetts Institute of Technology, <http://lancet.mit.edu/ga/>
- ²⁶Y. Chen, R. S. Berns, L. A. Taplin, and F. H. Imai, "A multi-ink color-separation algorithm maximizing color constancy", *Proc., IS&T/*

- SID 11th Color Imaging Conference* (IS&T, Springfield, VA, 2003) pp. 277–281.
- ²⁷R. Bala, “Device characterization”, *Digital Color Imaging Handbook* G. Sharma, Ed. (CRC Press, Boca Raton, FL, 2003) Chap. 5.

- ²⁸R. Schettini, D. Bianucci, G. Mauri, and S. Zuffi, “An empirical approach for spectral color printers characterization”, *Proc. 2nd European Conference in Color, Graphics, Imaging, and Vision, CGIV* (IS&T, Springfield, VA, 2004) pp. 393–397.